NOTATION

A_n, B_n, E, F, T = constants as defined by Equation (24)
c = constant as defined by Equation (1), cm.
e = Napierian logarithm base, dimensionless
g = acceleration due to gravity, cm./sec.^{2}
i = $\sqrt{-1}$
J = Jacobian as defined by Equation (31)
k = power law model parameter, (dyne) (sec.^{n})/sq. cm.
m = variable as defined by Equation (48), dimensionless
n = power law model parameter, dimensionless
P = pressure, dynes/sq.cm.
$P_m(Z)$ = Legendre's polynomials of the first kind
Q = flux, flow rate, cc./sec.
R = inner radius of fall tube, cm.
S = constant as defined by Equation (37)
u = fluid velocity, cm./sec.
v_o = terminal velocity of falling cylinder, cm./sec.
$\langle v_z \rangle$ = average fluid velocity, cm./sec.
x, y, z = space coordinates, cm.
Z = variable as defined by Equation (47), dimensionless

Greek Letters

α, β = dimensionless radii of inner and outer surfaces of the falling cylinder viscometer (eccentric case)
$(\Delta P/L)$ = pressure gradient, dynes/cc.
ϵ = eccentricity, cm.
κ = ratio of cylinder radius to inner radius of fall tube, dimensionless
μ = Newtonian viscosity, g./(cm.) (sec.)
ξ, η = bipolar coordinates
ρ = fluid density, g./cc.
ρ_o = cylinder density, g./cc.
τ_w = shear stress at the wall, dynes/sq.cm.
$\langle \tau_w \rangle$ = average shear stress at the wall, dynes/sq.cm.
ϕ = eccentricity ratio, as defined by Equation (10), dimensionless
Ψ_e = terminal velocity ratio in falling cylinder viscometer, dimensionless
Ψ_e' = terminal velocity ratio in annulus, dimensionless

LITERATURE CITED

1. Ashare, Edward, R. B. Bird, and J. A. Lescarboura, *AIChE J.*, **11**, 910-916 (1965).
2. Caldwell, J., *J. Roy. Tech. Coll. Glassgow*, **2**, 203-220 (1933).
3. Chen, M. C. S., M.S. thesis, Univ. Kansas, Lawrence (1967).
4. Eichstadt, F. J., and G. W. Swift, *AIChE J.*, **12**, 1179-1183 (1966).
5. Heyda, J. F., *J. Franklin Inst.*, **267**, 25-34 (1959).
6. Lescarboura, J. A., Ph. D. thesis, Univ. Kansas, Lawrence (1967).
7. ———, F. J. Eichstadt, and G. W. Swift, *AIChE J.*, **13**, 169-173 (1967).
8. Lindgren, E. R., *Tech. Rep. No. 3, Coll. Eng.*, Oklahoma State Univ., Stillwater (Oct. 1965).
9. Lohrenz, John, G. W. Swift, and Fred Kurata, *AIChE J.*, **6**, 547-550 (1960).
10. Piercy, N. A. V., M. S. Hooper, and H. F. Winny, *Phil. Mag.*, (Ser. 7), **15**, 647-675 (1933).
11. Snyder, W. T., and G. A. Goldstein, *AIChE J.*, **11**, 462-465 (1965).
12. Vaughn, R. D., *Soc. Petrol. Eng. J.*, **5**, 277-280 (1965).

Manuscript received February 16, 1967; revision received May 29, 1967; paper accepted May 31, 1967.

Effect of Pressure Gradient on Sonic-Point Heat Transfer

ELIYAHU TALMOR

Rocketdyne, Canoga Park, California

An analytical investigation of gas side heat transfer in high contraction, high convergence flows is presented. A partial criterion for retransition of a turbulent boundary layer is derived from the integral momentum equation and the effect of pressure gradient in the turbulent boundary-layer flow regime is described with the help of external flow relations. The validity of the analytical results is demonstrated by comparison to available internal and external flow, throat heat transfer data.

Accordingly, various turbulent boundary-layer heat transfer levels are obtained depending on the sonic-point pressure gradient, the specific heat ratio, the reference-to-stagnation temperature ratio, and the exponent of the viscosity-temperature function. Furthermore, the pressure gradient and the superficial mass velocity have opposite effects on the onset of retransition of a turbulent boundary layer.

In recent years there has been a considerable interest in compact combustors. Short combustion lengths offer substantial improvements in weight and cost. However, successful operation of such combustors requires knowledge of the heat transfer characteristics associated with the design aspects involved.

Compact combustors require relatively high flow-area contraction ratios, high convergence angles, and high wall curvatures at the throat, that is, the throat region is subjected to relatively high pressure gradients.

The effect of pressure gradient on heat transfer is complicated and diversified. In some range of Reynolds numbers and/or Mach numbers, increasing the pressure gradient tends to suppress the heat transfer level through the well observed phenomenon of reverse transition (*1* to *6*), while at the higher range of Reynolds numbers and/or

Mach numbers an increase in pressure gradient raises the corresponding turbulent boundary-layer heat transfer level (*7, 8*). Thus the study of heat transfer characteristics under these circumstances involves all three boundary-layer flow regimes: laminar, transitional, and turbulent.

Occasionally the requirement of deep throttling entails multiflow regime heat transfer regardless of the pressure gradient involved. In this case the boundary-layer transition is of the forward type governed by such factors as free-stream turbulence and wall roughness.

To elucidate the heat transfer characteristics involved, analytical efforts were undertaken to determine throat heat transfer as affected by the rate of acceleration (pressure gradient). The integral momentum equation is used to derive a partial criterion for retransition of a turbulent boundary layer, and the effect of pressure gradient on heat transfer in the turbulent boundary-layer flow regime is analyzed by analogy to external flow situations. Available internal and external flow, throat heat transfer data are accordingly recorrelated.

As will be shown, the results confirm the retransition criterion and extend the applicability of an external flow, high-pressure–gradient turbulent heat transfer relation (*7* to *9*) to internal flow, rectangular throat situations.

GENERAL CONSIDERATIONS

Forced convection normally controls the throat heat transfer mode in high-temperature combustors. Available relations for estimating convective heat transfer vary from simplified pipe flow forms (*10, 11*) to complex boundary-layer solutions (*12, 13*). However, the simplest and the most complex equations often yield close agreement particularly in the throat region (*14*). Even when in disagreement, the various heat transfer relations for a given boundary-layer flow regime are not necessarily contradictory. They yield various possible heat transfer levels for the given boundary-layer flow regime (*15*), with each level corresponding to a certain free-stream turbulence intensity, pressure gradient, wall roughness, or a combination thereof. In the treatment to follow simplified forms are employed to designate the various possible heat transfer levels for each boundary-layer flow regime considered. This is done for convenience only and should not be construed as a recommendation for the ultimate use of simplified heat transfer relations rather than boundary-layer solutions. Furthermore, whenever a more complex boundary-layer solution is involved, its transformation to a comparable simplified form will be attempted.

The major uncertainty involved in the prediction of throat heat transfer coefficients in high-temperature combustors is the choice of a reference temperature for evaluating the gas transport properties. The use of a film temperature (arithmetic average of the gas static temperature and the wall temperature) is still generally used despite the improved results reported by use of the static temperature (*14*), the stagnation temperature (*16*), or the arithmetic average of the adiabatic wall temperature and the actual wall temperature (*7, 8, 17*). The use of a film temperature based on the static gas temperature and the wall temperature will be adhered to herein, again for convenience so as to allow direct comparison to commonly used heat transfer relations (where such a reference temperature is employed).

While the choice of reference temperature pertains to simplified as well as complex boundary-layer solutions, the latter are also subjected to the uncertainty as to the starting point for a boundary-layer analysis. The injector face is certainly not the point at which a wall boundary-layer starts to develop, since a finite chamber length is required to complete combustion and the further downstream the boundary layer is assumed to start (shorter development lengths), the higher is the computed throat heat transfer coefficient, particularly when relatively short combustion chambers are involved.

In some respects the features of a high-convergence throat simplify throat boundary-layer analysis. A small radius of wall curvature in combination with high contraction and high degree of convergence results in a striking analogy to external flow throats. For example, a high contraction, high convergence, rectangular throat can be considered as an evolution of the case of flow between two throat tubes (*8, 9*). Furthermore, the effect of changing the degree of convergence in the two-dimensional internal flow throat is analogous to the effect of changing the throat body shape in external flow situations (*7*). Therefore, with minor modifications, boundary-layer equations or correlations developed for the external flow throat bodies (*8, 9*) should be applicable to the corresponding internal flow throats. This analogy will be proven useful in all boundary-layer flow regimes: laminar, transitional, and turbulent.

LAMINAR FLOW REGIME

A laminar boundary layer is seldom encountered in high-density combustors. In most applications the turbulent boundary layer and, more recently, the transitional boundary layer are of primary concern. However, determination of proper laminar heat transfer levels is essential for defining transitional flow regimes (*9*), even when a laminar boundary layer is not actually encountered.

An experimental investigation of laminar heat transfer in the throat region of an arc heated, low density wind tunnel was conducted by Carden (*18*). Experimental values obtained with nitrogen at stagnation temperatures of 5,200° to 6,500°R. and stagnation pressures of 0.9 to 1.5 atm. were compared with laminar predictions of several analytical procedures resulting in good agreement with the method of Cohen and Reshotko (*19, 20*).

Laminar heat transfer coefficients at higher densities are reported by Brinsmade and Desmon (*15*) for the throat region of a solid propellant rocket motor operating at stagnation pressures between 158 and 298 lb./sq.in.abs. They correlated their data by a Pohlhausen type of equation which takes the form

$$(N_{Nu})_r/(N_{Pr})^{0.4} = 0.290(N_{Re})_r^{0.5} \qquad (1)$$

where the gas density, viscosity, and thermal conductivity are all evaluated at the film temperature (average of the static gas temperature and the gas side wall temperature). The laminar heat transfer level described by Equation (1) is often higher than might be predicted by the more complex boundary-layer solutions (*12, 19, 20*) when applied to axisymmetric combustors at throttled conditions. However, Equation (1) was found to underestimate the laminar throat heat transfer levels of immersed throat bodies (*8, 16*) and throttled throats operating at pressure gradients approaching those encountered with external flow throat bodies (*7, 8, 16*).

Laminar throat heat transfer levels at extreme pressure gradients were derived from experimental pressure distributions around immersed throat tubes (*8, 16*). While a laminar boundary layer was not actually encountered at the sonic point on the immersed tubes, the laminar heat transfer levels developed therein (*8, 16*) were successfully used (*9*) in determining the transitional flow regime and the corresponding combustion induced, free-stream turbulence intensity for the propellant combination of N_2O_4/50% N_2H_4—50% UDMH. The basic relation describing laminar heat transfer around throat tubes is given (*16*) as

$$\frac{(N_{Nu})_{D,o}}{(N_{Pr})^{1/3}}\left[\frac{(N_{Ma})_\infty}{(N_{Re})_{D,o,\infty}}\right]^{1/2} = 3.75\left(\frac{2}{\gamma-1}\right)^{1/4}\frac{z^{1/2}}{\left[\int_0^\Lambda \left(\frac{p_e}{p_o}\right)^{\frac{m(\gamma-1)+1}{\gamma}} z^{1/2}\,d\Lambda\right]^{1/2}} \quad (2)$$

where

$$z = \left[\frac{p_e}{p_\infty}\right]^{\frac{\gamma-1}{\gamma}}\left[\left(\frac{p_o}{p_e}\right)^{\frac{\gamma-1}{\gamma}} - 1\right]$$

Equation (2) allows calculation of local heat transfer values from experimental angular pressure distribution data (*8, 16*). For the sonic point on small (*8*) and large (*16*) diameter throat tubes placed at area contraction ratios of 4 and 3, respectively, Equation (2) yields ($\gamma = 1.2$; $m = 0.6$)

$$\frac{(N_{Nu})_{D,o}}{(N_{Pr})^{1/3}}\left[\frac{(N_{Ma})_\infty}{(N_{Re})_{D,o,\infty}}\right]^{1/2} = 0.649 \quad (3)$$

Equation (3) can be made applicable to internal flow throats if expressed in terms of an internal flow dimension rather than the external flow dimension of throat tube O.D. By using the equivalent diameter of the gap between throat tubes (four times the ratio of wetted area to wetted perimeter) and by evaluating properties at the film temperature, Equation (3) leads to separate relations for each one of the two geometries involved (*8, 16*). For the 1.25 in. O.D. throat tube placed at an area contraction ratio of 3 (*16*), we have

$$(N_{Nu})_r/(N_{Pr})^{1/3} = 0.526(N_{Re})_r^{1/2} \quad (4)$$

and for a 0.375 in. O.D. throat tube placed at an area contraction ratio of 4 (*8*)

$$(N_{Nu})_r/(N_{Pr})^{1/3} = 0.614(N_{Re})_r^{1/2} \quad (5)$$

Equations (4) and (5) represent two laminar rectangular throat heat transfer levels, each corresponding to a different gas-side pressure gradient. The sonic-point pressure gradient $-d(p_e/p_o)/dx$ is 1.18 in.$^{-1}$ for Equation (4) and 4.10 in.$^{-1}$ for Equation (5).

Another calculation procedure for high favorable pressure gradients is given by Reshotko (*20*) with properties evaluated at the wall temperature. Applying Reshotko's procedure to the pressure distribution around the 1.25 in. O.D. throat tube placed at an area contraction ratio of 3 (*16*) and expressing the results in terms of the equivalent diameter of the rectangular throat with properties evaluated at the film temperature, we obtain

$$(N_{Nu})_r/(N_{Pr})^{0.4} = 0.475(N_{Re})_r^{1/2} \quad (6)$$

The heat transfer coefficients predicted by Equation (6) are 16% lower than those predicted by Equation (4), even though both equations were derived on the basis of the same experimental pressure distribution (*16*).

TRANSITIONAL FLOW REGIME

Two types of boundary-layer transition may be encountered at the sonic region of high-temperature combustors: forward and reverse. In the forward case, the boundary layer is transitional at the sonic point while tending to be laminar upstream towards the injector face and turbulent downstream towards the nozzle exit. In the reverse case, the boundary layer is transitional at the sonic point (where the pressure gradient is maximum) while tending to be turbulent upstream and downstream of this point where

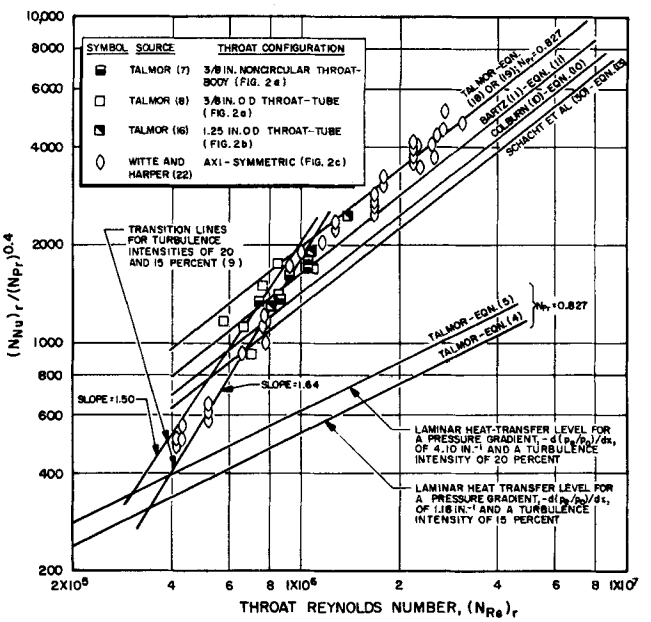

Fig. 1. Transitional and turbulent boundary-layer heat transfer at the sonic points of rectangular and axisymmetric throats with the propellant combinations of $N_2O_4/50\%N_2H_4$—50% UDMH (*7, 8, 16*) and N_2O_4/N_2H_4 (*22*).

lower pressure gradients exist. The boundary-layer flow regimes thus encountered starting at the convergence section of the combustor are turbulent-transitional-turbulent. Seldom (*6, 21*) does the retransition process involve a laminar boundary layer.

Forward transition at the sonic region of high-temperature combustors has been observed with external (*8, 9, 16*) and internal (*22*) flow throat configurations. The main factors affecting such transition are the combustion induced free-stream turbulence, the pressure gradient, and the degree of wall cooling (T_w/T_o). While suitable theories of boundary-layer transition are available (*23, 24*), their application is limited mainly because the free-stream turbulence intensity associated with the combustion processes of the various propellant combinations is not known.

Recently (*9*), successful determination of combustion induced, free-stream turbulence intensities was accomplished by using transitional immersed cylinder heat transfer measurements (*8, 16*) in conjunction with the theory of boundary-layer transition of van Driest and Blummer (*23*). Accordingly (*9*), the combustion induced turbulence intensity of the nitrogen tetroxide-50% unsymmetrical dimethyl hydrazine/50% hydrazine propellant combination is at least 15 to 20% depending on distance along the convergence section of the combustion chamber.

The immersed throat tube heat transfer data (*8, 16*) and their associated 20 and 15% turbulence-intensity transition lines (*9*) are presented in Figure 1, where the Nusselt and Reynolds numbers are expressed in terms of the equivalent diameter of the rectangular gaps between throat tubes or between a throat tube and its confining chamber walls. Similarly, noncircular throat body heat transfer results (*7*) and sonic-point heat transfer measurements in a circular combustor (*22*) are also presented. In all cases the data represent peak heat transfer values as reported for the sonic point upstream of the geometric throat. The corresponding throat configurations are schematically illustrated in Figure 2.

The heat transfer data of Figure 1 cover a wide range of chamber lengths and area contraction ratios. The noncircular and circular throat body heat transfer measure-

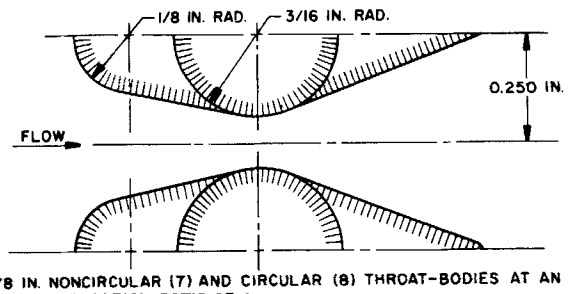

(a) 3/8 IN. NONCIRCULAR (7) AND CIRCULAR (8) THROAT-BODIES AT AN AREA CONTRACTION RATIO OF 4.

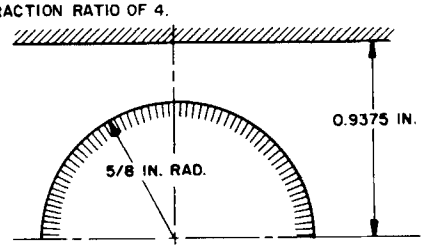

(b) 1.25 IN. OD THROAT-TUBE AT AN AREA CONTRACTION RATIO OF 3 (16).

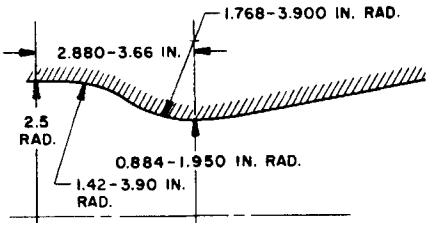

(c) AXI-SYMMETRIC TANGENT-ARCS THROAT AT AREA CONTRACTION RATIOS OF 1.64 TO 8 (22).

Fig. 2. External and internal flow throat configurations with the propellant combinations of N_2O_4/50%N_2H_4—50% UDMH (7, 8, 16) and N_2O_4/N_2H_4 (22).

ments (7, 8, 16) were taken at area contraction ratios of 4 and 3 and chamber lengths of 6 and 23 in. No specific convergence angle can be associated with these data since the convergence of an arc is variable, dropping from 90 deg. at the stagnation point to essentially zero at the sonic point.

The data of Witte and Harper (22) were obtained at area contraction ratios in the range of 1.64 to 8 and chamber lengths of 8 to 12 in. The propellant combination in this case was N_2O_4/N_2H_4, similar to the N_2O_4/50% N_2H_4-50% UDMH propellant combination used with the immersed throat body configuration. Therefore, the combustion induced turbulence intensity should be comparable for all data given in Figure 1, and if the pressure gradients are also camparable, a common transitional Reynolds number range should be obtained. In accordance with Figure 1, this is really the case; that is, the transitional throat heat transfer data obtained with the propellant combination of N_2O_4/N_2H_4 (22) follow the 20 and 15% turbulence intensity lines derived (9) on the basis of throat tube heat transfer measurements (8, 16) with the propellant combination of N_2O_4/50% N_2H_4-50% UDMH. Furthermore, mutual agreement among the various sets of data (8, 16, 22) also exists in the turbulent boundary-layer flow regime.

The free-stream turbulence intensity does not always govern boundary-layer transition. In some cases it is either not present (6), or it is counteracted by a highly negative pressure gradient and/or wall cooling (21). In fact, an overriding effect of these parameters may lead to the phenomenon of reverse transition.

Generally, the factors which tend to stabilize a laminar boundary layer also promote retransition, that is, high favorable (negative) pressure gradients, low Reynolds numbers, and increased wall cooling. This is well reflected by the heated air experiments of Back et al. (6) and the ambient wind tunnel experiments of O'Brien (21). Both investigations were conducted at comparable throat pressure gradients, for example, $-d(p_e/p_o)/dx$ of 0.709 and 0.608 in.$^{-1}$, respectively.

Back et al. (6) measured convective heat transfer rates in a convergent-divergent circular nozzle operating at stagnation pressures of 30 to 250 lb./sq.in.abs., stagnation temperatures of 1,030° to 2,000°R., and wall-to-stagnation temperature ratios of 0.35 to 0.80. Their results showed that at the lower stagnation pressures the boundary layer underwent transition from a turbulent profile at the nozzle entrance to a laminar profile at the sonic point; that is, an increase in pressure gradient promotes retransition.

O'Brien (21) reports local heat transfer coefficients for two rectangular throat configurations resembling flow between a cylinder and a flat wall (16). With a given pressure gradient and a free-stream Reynolds number, retransition of the throat boundary layer was accomplished by increased wall cooling, for example, by systematically decreasing the wall-to-stagnation temperature ratio in the range of 0.90 to 0.50. The results of the laminarization attempts of O'Brien (21) are graphically presented in Figure 3 along with the heated air results of Back et al. (6). As shown, complete retransition to a laminar boundary layer occurred at Reynolds numbers between 500,000 and 800,000. At the other two Reynolds number ranges at which laminarization was attempted, the retransition of the boundary layer was not complete.

It is of interest to note that the throat-wall cooling effect in O'Brien's experiments apparently counteracted free-stream turbulence intensities as high as 30% at the entrance to the convergence section. However, indications are that the effect of wall cooling on laminarization reverses itself at a wall-to-stagnation temperature ratio of approximately 0.3, particularly at the higher Mach numbers (21, 25).

High-temperature combustors generally operate at a wall-to-stagnation temperature ratio of approximately 0.3 with no freedom of variation of this parameter. Therefore, retransition of throat boundary layers can only be accomplished by increasing the throat pressure gradient (varying the throat configuration) provided that the Reynolds number is sufficiently low.

The suppression of heat transfer rates by flow acceleration, while well observed, is not fully understood. Pertinent water table observations by Schraub (4) indicate that flow acceleration reduces the frequency at which turbulence eddies leave the wall. The turbulence bursts frequency was related to a dimensionless acceleration parameter $K = (\nu/u_e^2)(du_e/dx)$, and it was observed (4) that the turbulence bursts from the wall disappeared at $K \cong 3.5 \times 10^{-6}$.

Moretti and Kays (26) report an experimental investigation of heat transfer to a turbulent boundary layer at various rates of free-stream acceleration ($0 < K < 4 \times 10^{-6}$). An empirical correlation of the depression of heat transfer with flow acceleration is presented. At $K > 3.3 \times 10^{-6}$, the heat transfer level was close to that predicted for a laminar boundary layer assumed to originate at the entrance to the acceleration zone. This seems to be consistent with the visual observation of Schraub (4).

RETRANSITION CRITERION

A criterion for retransition of a turbulent boundary layer can be derived from the integral momentum equation. In terms of a modified Stewartson coordinate system (27), the integral momentum equation for a compressible turbulent boundary layer on an infinite wall can be written

as follows:

$$\frac{d\bar{\theta}}{dX} + \frac{1}{U_e}\frac{dU_e}{dX}(2\bar{\theta} + \delta^*) = \frac{\bar{\tau}_x}{\rho_o U_e^2} \qquad (7)$$

where

$$\bar{\theta} = \int_0^{\bar{\delta}} \left[\frac{U}{U_e} - \left(\frac{U}{U_e}\right)^2\right] dY$$

$$X = \int_0^x \frac{\rho_r \mu_r}{\rho_o \mu_o}\sqrt{\frac{T_e}{T_o}}\, dx$$

$$U_e = \sqrt{\frac{T_o}{T_e}}\, u_e$$

$$\delta^* = \int_0^{\bar{\delta}} \left(1 - \frac{U}{U_e}\right) dY$$

$$\bar{\tau}_x = \frac{\rho_o \mu_o}{\rho_r \mu_r}\left(\frac{T_o}{T_e}\right) \tau_x$$

$$Y = \sqrt{\frac{T_e}{T_o}}\int_0^y \frac{\rho}{\rho_o}\, dy$$

When one assumes a one-seventh power velocity profile in the boundary layer, $\delta^*/\bar{\theta} = 1.286$ and the shear stress is $\bar{\tau}_x/\rho_o U_e^2 = 0.0128\ (\nu_o/U_e\,\bar{\theta})^{1/4}$. Substituting in Equation (7) and multiplying and dividing the second term on the left side by U_e/ν_o, one gets

$$\frac{d\bar{\theta}}{dX} + 3.286\,(N_{Re})_{\bar{\theta}}\frac{\nu_o}{U_e^2}\frac{dU_e}{dX} = \frac{0.0128}{(N_{Re})_{\theta}^{1/4}}$$

On the basis of the contention that the factors affecting forward transition also affect reverse transition (*21*), it is reasonable to assume that the onset of retransition will occur when $(N_{Re})_{\theta}$ is reduced (by flow acceleration) to the same critical value of 360 suggested (*28*) for transition in the forward direction. Substituting $(N_{Re})_{\bar{\theta}} = 360$ and solving for $d\bar{\theta}/dX$ one gets

$$\frac{d\bar{\theta}}{dX} = 0.00294 - 1{,}183\frac{\nu_o}{U_e^2}\frac{dU_e}{dX}$$

However, for $(N_{Re})_{\bar{\theta}}$ to fall below the critical value, $(d\bar{\theta}/dX)$ must be negative. Thus

$$1{,}183\left(\frac{\nu_o}{U_e^2}\right)\frac{dU_e}{dX} > 0.00294$$

or

$$\left(\frac{\nu_o}{U_e^2}\right)\frac{dU_e}{dX} > 2.48 \times 10^{-6} \qquad (8)$$

which is in good agreement with the results of Launder (*5*) and Moretti and Kays (*26*).

Transformation to conventional coordinates results in

$$dU_e = \sqrt{\frac{T_o}{T_e}}\left[\frac{4 + 2N_{Ma}(\gamma - 1)}{4 + 3N_{Ma}(\gamma - 1)}\right] du_e$$

$$U_e^2 = \frac{T_o}{T_e}u_e^2$$

$$dX = \frac{\rho_r \mu_r}{\rho_o \mu_o}\sqrt{\frac{T_e}{T_o}}\, dx$$

so that the criterion for retransition becomes

$$\left[\frac{4 + 2N_{Ma}(\gamma - 1)}{4 + 3N_{Ma}(\gamma - 1)}\right]\left(\frac{\mu_o}{\mu_r}\right)^2\left(\frac{\nu_r}{u_e^2}\right)\frac{du_e}{dx}$$

$$> 2.48 \times 10^{-6} \qquad (8a)$$

Rewriting the flow acceleration parameter in terms of the local pressure gradient, Reynolds number, and Mach number, one obtains

$$\frac{(p_o/p_e)}{(N_{Re})_r N_{Ma}^2}\left[-d_h\frac{d(p_e/p_o)}{dx}\right] > 2.48(10^{-6})\left[\frac{4 + 2N_{Ma}(\gamma - 1)}{4 + 3N_{Ma}(\gamma - 1)}\right]\left(\frac{T_r}{T_o}\right)^{2m}\gamma \qquad (9)$$

In accordance with Schraub (*4*), the pressure gradient decreases the turbulence production at the wall. However, the turbulence at a given point in the boundary layer is generated at various points upstream, so that a heat transfer depression may be encountered downstream of the region of high flow acceleration (*26*). It is therefore not clear at what point in a convergence section should a retransition criterion be applied to check the possibility of reverse transition at the sonic point. Kays (*28*) suggests 200 momentum thicknesses upstream the point of interest.

Equation (9) indicates that at a given Mach number, the pressure gradient and the superficial mass velocity have opposite effects on the onset of retransition. A mild offsetting effect of wall cooling is reflected by Equation (9), since for a given stagnation temperature the Reynolds number based on film properties tends to increase with wall cooling (Figure 3). However, the offsetting effect of free-stream turbulence intensity is absent in the retransition criterion so that its application to high-temperature combustors is somewhat limited. Furthermore, the retransition criterion defined by Equation (9), while written in terms of the equivalent diameter, is not applicable for an axisymmetric nozzle. In this respect application to rectangular throats of high-temperature combustors should be valid provided that the actual local pressure gradient and the combustion induced, free-stream turbulence intensity (if any) are both known.

TURBULENT FLOW REGIME

The earliest form of a fully turbulent heat transfer relation is that of Colburn (*1*) for moderate temperature differences:

$$(N_{Nu})_r/(N_{Pr})^{0.4} = 0.023\,(N_{Re})_r^{0.8} \qquad (10)$$

Bartz (*11*) extended the application of Equation (1) to high-temperature combustors by introducing gas transport properties at the film temperature (average of the gas static and wall temperatures) and changing Colburn's constant from 0.023 to 0.026; that is

$$(N_{Nu})_r/(N_{Pr})^{0.4} = 0.026\,(N_{Re})_r^{0.8} \qquad (11)$$

Equation (11) has found wide application because of its simplicity and its frequent good agreement with experimental data and the more complicated boundary-layer solutions (*12, 13*), particularly at the sonic point of high-temperature combustors (*14*).

Kutateladze and Leontev (*29*) apply a theory of the limiting law of heat transfer to correct Colburn's equation to the form

$$(N_{Nu})_o/(N_{Pr})^{0.4} = 0.023\,(N_{Re})_o^{0.8}\left[\frac{2}{(T_w/T_e)^{1/2} + 1}\right]^2 \qquad (11a)$$

where the properties in $(N_{Nu})_o$, N_{Pr} and $(N_{Re})_o$ are evaluated at the mixing-cup temperature of the stream (stagnation temperature). The introduction of the cor-

rection factor $\{2/[(T_w/T_e)^{1/2} + 1]\}^2$ helped correlate convective heat transfer results in the critical region for water, carbon dioxide, and oxygen. For typical high-temperature combustion applications (for example, $T_w/T_e \sim 0.3$), Equations (11*a*) and (11) yield identical results.

A pertinent investigation of gas side heat transfer in a liquid oxygen/gaseous hydrogen combustor is reported by Schacht et al. (*30*). The nozzle used had a 5-in. diameter throat, area contraction ratio of 4.64 and a convergence angle of 30 deg. A dish shaped coaxial injector was employed with the throat placed 14.5 in. from the injector face. Transient temperature measurements at five axial locations were reduced to local heat transfer coefficients, and the latter were empirically correlated in a form similar to Equation (11).

The results showed that one constant in the form of Equation (11) could not correlate the data for all axial locations over the Reynolds number range investigated (corresponding to a chamber pressure range of 150 to 1,000 lb./sq.in.abs.). The values of the constant (with N_{Pr} taken to the power of 0.3 rather than 0.4) varied from a high of 0.026 to a low of 0.015 at the geometric throat. However, inspection of the reported heat transfer profiles (*30*) reveals peak values upstream of the geometric throat at an area contraction ratio of approximately 1.5. At this point the constant of the equation is 0.020; that is

$$(N_{Nu})_r/(N_{Pr})^{0.3} = 0.020\ (N_{Re})_r^{0.8} \qquad (12)$$

Adjusting to a Prandtl number to a power of 0.4, one gets

$$(N_{Nu})_r/(N_{Pr})^{0.4} = 0.021\ (N_{Re})_r^{0.8} \qquad (13)$$

The throat pressure gradient associated with Equation (13) was not measured (*30*). However, as shown in Figure 3, Equation (13) fits the heated air heat transfer data of Back et al. (*6*) obtained in a similar throat operating at a throat pressure gradient $-d(p_e/p_o)/dx$ of 0.709 in.$^{-1}$ and an apparently negligible free-stream turbulence intensity (though not measured). Conceivably, a moderate combustion induced, free-stream turbulence intensity in the case of Schacht et al. (*30*) could decay towards the sonic point with the relatively long combustion chamber employed.

Effect of Pressure Gradient

Turbulent boundary-layer heat transfer rates at high-pressure gradients were encountered at the sonic points on immersed noncircular and circular throat bodies (*7, 8, 16*). Corresponding heat transfer levels were derived from experimental pressure distribution around immersed throat tubes (*8, 16*), and the resulting relations were successfully used for correlating actual throat heat transfer data and predicting the effect of pressure gradient on throat heat transfer in the turbulent boundary-layer flow regime (*7*).

The basic relation describing turbulent heat transfer around throat tubes is given (*16*) as

$$\frac{(N_{Nu})_{D,o}}{(N_{Pr})^{1/3}}\left[\frac{(N_{Ma})_\infty}{(N_{Re})_{D,o}}\right]^{0.40}\left(\frac{\mu_o^2}{g_c\rho_o D^2 p_o}\right)^{0.20}\left(\frac{T_r}{T_o}\right)^{0.80(1-m)} = 0.09272\left[\frac{2}{\gamma-1}\right]^{0.20}\left[\frac{z}{(p_o/p_e)^{4-1/\gamma}}\right]^{0.20}\left[\frac{-d(p_e/p_o)}{d\Lambda}\right]^{0.20} \qquad (14)$$

where z is a local pressure-ratio function defined in conjunction with Equation (2).

Equation (14) is a solution of the integral momentum equation for an infinite cylinder [Equation (7)] with Colburn's analogy and a one seventh-power law velocity profile assumed. It allows calculation of local heat transfer coefficients from experimental pressure distribution data (*8, 16*). To make it applicable to internal flow configurations, the pressure gradient term has to be expressed in terms of a linear distance from stagnation (or distance from the start of convergence) and the external flow dimension D has to be replaced with an internal flow dimension such as the equivalent diameter of the gap between the throat tubes (*8*) or between a throat tube and its confining chamber wall (*16*). With the further manipulation of expressing all transport properties at the reference temperature and rearranging variables, one obtains

$$\frac{(N_{Nu})_r}{(N_{Pr})^{1/3}(N_{Re})_r^{0.80}} = 0.03594\left[\frac{\gamma-1}{2\gamma}\right]^{0.20}\left(\frac{p_o}{p_e}\right)^{1/5\gamma}\left(\frac{d_h}{z}\right)^{0.20}\left[\frac{-d(p_e/p_o)}{dx}\right]^{0.20}\left(\frac{T_r}{T_o}\right)^{0.6m} \qquad (15)$$

At the sonic point, the critical pressure ratio is given as

$$(p_e/p_o) = [2/(\gamma+1)]^{\gamma/(\gamma-1)} \qquad (16)$$

Substitution in Equation (15) yields

$$\frac{(N_{Nu})_r}{(N_{Pr})^{1/3}(N_{Re})_r^{0.80}} = 0.03594\left[\left(\frac{\gamma+1}{2}\right)^{\frac{\gamma}{\gamma-1}}\left(\frac{1}{\gamma}\right)\right]^{0.20}\left\{d_h\left[\frac{-d(p_e/p_o)}{dx}\right]\right\}_{N_{Ma}=1}^{0.20}\left(\frac{T_r}{T_o}\right)^{0.6m} \qquad (17)$$

Equation (17) permits evaluation of sonic-point heat transfer coefficients provided that the local pressure gradient is known for the gas stream in question. For example, for a 0.375 in. O.D. throat tube placed at an area contraction ratio of 4, where $d_h = 0.222$ in. and $-d(p_e/p_o)/dx = 4.10$ in.$^{-1}$ (*8*), a value of 0.0312 is obtained for the right-hand side of Equation (17). Similarly, a value of 0.0289 is obtained for a 1.25 in. O.D. throat tube placed at an area contraction ratio of 3, where $d_h = 0.560$ in. and $-d(p_e/p_o)\ dx = 1.18$ in.$^{-1}$ (*16*). From an average of the two results, a value of 0.0300 is obtained, while the combined actual throat heat transfer data of both investigations (*8, 16*) yield a value of 0.0313 for the right-hand side of Equation (17); that is

$$\frac{(N_{Nu})_r}{(N_{Pr})^{1/3}(N_{Re})_r^{0.80}} = 0.0313 \qquad (18)$$

Thus, Equation (17) underpredicts the constant on the right-hand side of Equation (18) by 4.5%. For comparison, the curved plate, turbulent boundary-layer heat transfer relation of Meyer (*12*) overpredicts this constant by 18%.

Equation (18) is superimposed on the rectangular and circular throat heat transfer results presented in Figure 1 ($\gamma = 1.2$, $N_{Pr} = 0.83$). While expectedly supported by the rectangular throat heat transfer data (*8, 16*) from which it was derived, Equation (18) also fits the turbulent boundary-layer heat transfer data of Witte and Harper (*22*) obtained at the sonic point of an axisymmetric

nozzle using a similar propellant combination.

Adjusting the constant in Equation (17) to yield Equation (18), we obtain

$$\frac{(N_{Nu})_r}{(N_{Pr})^{1/3}\,(N_{Re})_r^{0.80}} = 0.0375\left[\left(\frac{\gamma+1}{2}\right)^{\frac{\gamma}{\gamma-1}}\left(\frac{1}{\gamma}\right)\right]^{0.20}\left\{d_h\left[\frac{-d(p_e/p_o)}{dx}\right]\right\}_{NMa=1}^{0.20}\left(\frac{T_r}{T_o}\right)^{0.6m} \qquad (19)$$

Equation (19) is in proper form for application to any rectangular throat configurations where the sonic-point pressure gradient is known. For example, for the short radius nozzle of O'Brien (*21*), where $\gamma = 1.4$, $d_h = 0.546$ in., and $-d(p_e/p_o)/dx = 0.61$ in.$^{-1}$, Equation (19) predicts

$$\frac{(N_{Nu})_r}{(N_{Pr})^{1/3}\,(N_{Re})_r^{0.80}} = 0.0300 \qquad (20)$$

for a wall-to-stagnation temperature ratio of 0.9. As shown in Figure 3, Equation (20) fits the data of O'Brien (*21*) at the onset of his laminarization paths.

Equation (19) yields various turbulent boundary-layer heat transfer levels (various values for the right side of the equation) depending on the sonic-point pressure gradient, the specific heat ratio, the reference-to-stagnation temperature ratio, and the exponent of the viscosity-temperature function. In fact, the turbulent heat transfer levels of Colburn (*10*), Equation (10); Bartz (*11*), Equation (11); and Schacht et al. (*30*), Equation (13) are special cases of Equation (19) for smooth wall, rectangular throat applications.

For a given gas stream and throat size, Equation (19) shows that the associated turbulent boundary-layer heat transfer levels can be depressed by the reduction of the sonic-point pressure gradient. An experimental proof to this effect is provided by comparison of measured heat transfer rates to noncircular and circular throat bodies (*7*) having a ⅜-in. dimension in a cross flow of the same gas stream (Figure 2*a*). For both cases the dimensionless pressure gradient $-d(p_e/p_o)/d(x/L)$ was identical so that the increased body length L (distance between the stagnation and sonic points) associated with the noncircular shape (*7*) resulted in reduction of the sonic-point pressure gradient $-d(p_e/p_o)/dx$ from a value of 4.10 in.$^{-1}$ for the ⅜ in. circular throat body to a value of 1.95 in.$^{-1}$ for the ⅜ in. noncircular throat body (Figure 4*a*). In accordance with Equation (19), such a reduction in the throat pressure gradient should result in a 16% reduction of the sonic-point heat transfer coefficient; that is, the constant on the right-hand side of Equation (18) should decrease from a value of 0.0313 for the circular throat body to a value of 0.0270 for the noncircular throat body. This is supported by actual heat transfer measurements (*7*) as graphically presented in Figure 4*b*.

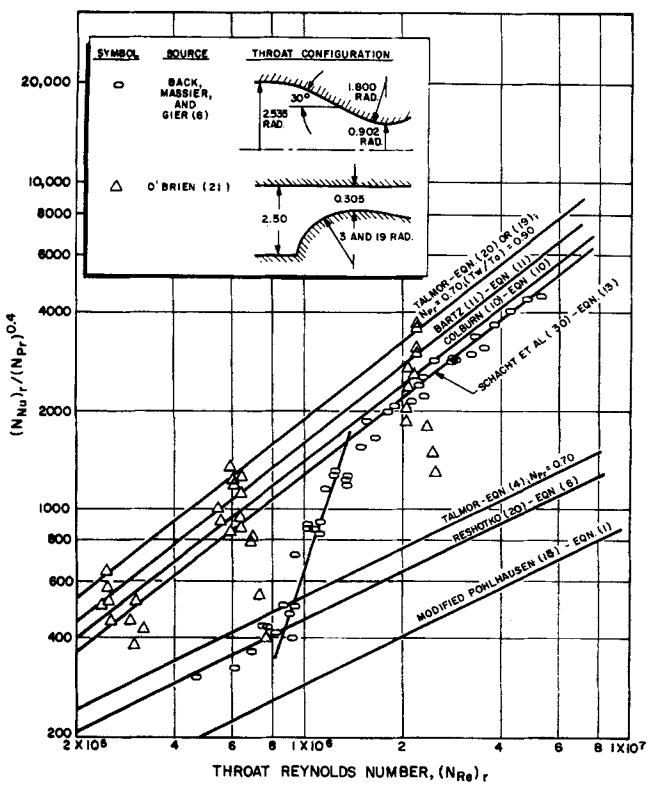

Fig. 3. Reverse transition at the sonic points of axisymmetric and rectangular throats operating with heated (*6*) and ambient (*21*) air streams, respectively; $0.35 < (T_w/T_o) < 0.90$.

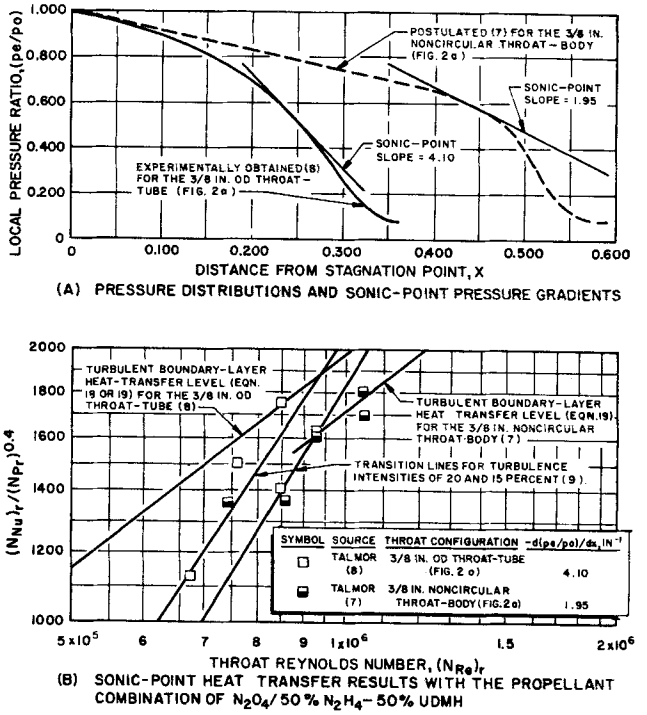

Fig. 4. Suppression of turbulent boundary-layer heat transfer rates by reduction of sonic-point pressure gradients in external flow throat configurations (*7*).

Changing to noncircular throat body shape in external flow configurations is analogous to decreasing the convergence angle in internal flow configurations. In both cases the length of the convergence section is thereby increased and the effect of wall curvature at the sonic point is decreased; that is, the tangency point between the converging ramp and the throat region wall curvature moves closer to the geometric throat as the convergence angle is decreased.

On this basis, the smaller the radius of wall curvature at the throat the more sensitive is the throat pressure gradient to variation in convergence angle. However, the effect of pressure gradient on throat heat transfer is rather diversified. Its decrease at the higher Reynolds number range results in reduced heat transfer rates, while at the lower Reynolds number range reduced pressure gradients might increase heat transfer rates through the promotion of a turbulent boundary layer where a transitional bound-

ary layer is otherwise encountered. This is further reflected by the results of heat transfer experiments with the propellant combination of liquid oxygen/gaseous hydrogen (*31*).

CONCLUSIONS

The pressure gradient and the superficial mass velocity have opposite effects on the onset of retransition of a turbulent boundary layer. A mild offsetting effect of wall cooling is also revealed by the retransition criterion derived from the integral momentum equation and confirmed by available experimental results (*5, 26*). However, the free-stream turbulence intensity is absent in the retransition criterion so that its application is somewhat limited.

The heat transfer behavior of high contraction, high convergence throats can be analyzed by analogy to external flow throat configurations. For example, an external flow turbulent boundary-layer heat transfer relation (7 to 9) was found applicable for describing the effect of pressure gradient on sonic-point heat transfer in internal flow, rectangular throat situations. Accordingly, various values for the ratio $(N_{Nu})_r/(N_{Pr})^{1/3}(N_{Re})_r^{0.80}$ are obtained depending on the sonic-point pressure gradient, the equivalent diameter, the specific heat ratio, the reference-to-stagnation temperature ratio, and the exponent of the viscosity-temperature function.

NOTATION

D = outside diameter of an immersed cylinder
d_h = equivalent diameter, four times the ratio of wetted area to wetted perimeter
g_c = conversion factor in Newton's law of motion, equals 32.2 (ft.)(lb. mass)/(sec.^{2})(lb. force)
K = acceleration parameter
k = thermal conductivity
m = gas viscosity-temperature exponent ($\mu \sim T^m$)
N_{Ma} = Mach number
N_{Nu} = Nusselt number
N_{Pr} = Prandtl number
N_{Re} = Reynolds number
p = pressure
T = absolute temperature
U = transformed velocity defined in conjunction with Equation (7)
u = velocity in the x direction
X = transformed coordinate defined in conjunction with Equation (7)
x = distance along the converging wall
Y = transformed coordinate normal to the wall, defined in conjunction with Equation (7)
z = pressure function defined in conjunction with Equation (2).

Greek Letters

γ = specific heat ratio
$\bar{\delta}$ = velocity boundary-layer thickness in transformed coordinate system [Equation (7)]
δ^* = integral thickness parameter defined in conjunction with Equation (7)
$\bar{\theta}$ = integral thickness parameter defined in conjunction with Equation (7)
Λ = angle, degrees from the forward stagnation point of an immersed cylinder
μ = gas viscosity
ν = kinematic viscosity
ρ = density
$\bar{\tau}$ = transformed shear stress defined in conjunction with Equation (7)

Subscripts

D = based on immersed cylinder O.D.
e = local conditions along the outer edge of the boundary layer
o = properties (k, μ, and ρ) at stagnation conditions
r = properties (k, μ, and ρ) at reference temperature
x = x direction
w = wall
$\bar{\theta}$ = based on $\bar{\theta}$
∞ = approach (velocity) to an immersed cylinder; start of convergence

LITERATURE CITED

1. Sergienko, A. A., and V. K. Gretsov, *Sov. Phys. Dokl.*, **4**, No. 2, 275 (1959).
2. Sennoo, Yasutoshi, *Trans. Am. Soc. Mech. Engrs*, **80**, 1711 (1958).
3. Wilson, D. G., and J. A. Pope, *Proc. Inst. Mech. Engrs. (London)*, **168**, 861 (1954)
4. Schraub, F. A., Ph.D. dissertation, Stanford Univ., Calif. (1965).
5. Launder, B. E., *Gas Turbine Lab. Rept. No. 77*, Mass. Inst. Technol., Cambridge (1964).
6. Back, L. H., P. F. Massier, and H. L. Gier, *Int. J. Heat Mass Transfer*, **7**, 549 (1964); *Tech. Rept. No. 32-415* (Rev. No. 1), Jet Propulsion Lab., Calif Inst. Technol., Pasadena (Feb., 1965).
7. Talmor, Eliyahu, Proceedings of the Third International Heat Transfer Conference, Vol. 1, p. 77, Chicago, Ill. (Aug., 1966).
8. Talmor, Eliyahu, Paper presented at Am. Inst. Chem. Engrs. San Francisco meeting, Calif. (May, 1965).
9. ———, *AIChE J.*, **12**, 1092 (1966).
10. Colburn, A. P., *Trans. Am. Inst. Chem. Engrs.*, **29**, 174 (1933).
11. Bartz, D. R., *Jet Propulsion*, **21**, No. 1, 49 (1957).
13. Elliott, D. G., D. R. Bartz, and S. Silver, *Tech. Rept. No. 32-387*, Jet Propulsion Lab., Calif. Inst. Technol., Pasadena (Feb., 1963).
14. Seader, J. D., and W. R. Wagner, *Chem. Eng. Progr. Symp. Ser. No. 52*, **60**, 130 (1964).
15. Brinsmade, A. F., and L. G. Desmon, *Chem. Eng. Progr. Symp. Ser. No. 59*, **61**, 88 (1965).
16. Talmor, Eliyahu, *ibid.*, 50.
17. ———, *Chem. Eng. Progr. Symp. Ser. No. 64*, **62**, 216 (1966).
18. Carden, W. H., *AIAA J.*, **3**, 2183 (1965).
19. Cohen, C. B., and Eli Reshotko, *Natl. Advisory Comm. Aeronaut. Rept. 1294* (1956).
20. Reshotko, Eli, *Natl. Advisory Comm. Aeronaut. Tech. Note 3888* (1956).
21. O'Brien, R. L., *Tech. Documentary Rept. No. AFRPL, TR-65-40*, Air Force Rocket Propulsion Lab., Edwards, Calif. (Feb., 1965).
22. Witte, A. B., and E. Y. Harper, *AIAA J.*, **1**, 443 (1963).
23. van Driest, E. R., and C. B. Blumer, *ibid.*, 1303.
24. Schlichting, Hermann, "Boundary Layer Theory," McGraw-Hill, New York (1960).
25. Richards, B. E., and J. L. Stollery, *AIAA J.*, **4**, 2224 (1966).
26 Moretti, P. M., and W. M. Kays, *Intern. J. Heat Mass Transfer*, **8**, 1187 (1965).
27. Beckwith, I. E., and J. J. Callagher, *Natl. Aeronaut. Space Admin. Tech. Rept. R-104* (1961).
28. Kays, W. M., "Convective Heat and Mass Transfer," McGraw-Hill, New York (1966).
29. Kutateladze, S. S., and A. I. Leontev, "Turbulent Boundary Layers in Compressible Gases," Academic Press, New York (1964).
30. Schacht, R. L., R. J. Quentmeyer, and W. L. Jones, *Natl. Aeronaut. Space Admin. Tech. Note D-2832* (June, 1965).
31. Talmor, Eliyahu, Paper presented at the Ninth Natl. Heat Transfer Conf., Seattle, Wash. (Aug., 1967).

Manuscript received January 11, 1967; revision received May 11, 1967; paper accepted May 15, 1967.